Double-scattering effects in depolarised light scattering spectrometry

1979 J. Phys. A: Math. Gen. 12 581

(http://iopscience.iop.org/0305-4470/12/4/017)

J. Phys. A: Math. Gen., Vol. 12, No. 4, 1979. Printed in Great Britain

Double-scattering effects in depolarised light scattering spectrometry

G Koopmans, P C Hopman and J Greve

Physics Laboratory of the Vrije Universiteit, De Boelelaan 1081, Amsterdam, The Netherlands

Received 30 March 1978, in final form 8 September 1978

Abstract. Measurements of rotational diffusion coefficients by depolarised light scattering spectrometry are often disturbed by double-scattering effects. These effects may be reduced by minimising the concentration of scatterers and by using an appropriate geometry. Such an optimum geometry is proposed.

Explicit expressions for the contribution of double scattering to the field correlation function are computed for the optimum geometry. The correlation functions evaluated numerically are compared with experimental data in the case of polystyrene latex spheres. The agreement is excellent.

The expressions derived can be used to correct correlation functions obtained experimentally in case double scattering cannot be avoided.

1. Introduction

In the last few years dynamic light scattering has become a major technique for the determination of translational diffusion coefficients. This method may also be used to obtain rotational diffusion coefficients of optically anisotropic molecules, when one usually measures the depolarised scattered intensity.

At the present time, there have been few experimental studies of this subject (Sorenson *et al* 1976). This is probably due to to the fact that macromolecular optical anisotropies are usually small relative to the average molecular polarisabilities. The depolarised intensity is then very weak, and severe demands are imposed on the experimental set-up. A way to obtain measurable intensities could be the use of concentrated solutions. However, the high concentrations give rise to multiple scattering. This contributes to the depolarised intensity even in the case of optically isotropic particles. It is therefore very often impossible to measure the correlation function of the depolarised component due to single scattering separately. Similar arguments hold if intramolecular movements are to be studied.

To overcome this problem we calculated explicit expressions for the correlation functions of the depolarised component due to double scattering, using a practical scattering geometry. The equations derived were verified experimentally by measurements on solutions of polystyrene latex spheres. It could be shown that the agreement between experiment and theory is excellent. The expressions derived can be used to correct correlation functions obtained experimentally in case double scattering cannot be avoided.

0305-4470/79/040581+10$01.00

It appears that the relative contributions of single and double scattering to the depolarised intensity measured by the detector are strongly dependent on the scattering geometry. We therefore propose an experimental set-up that minimises the contribution of double scattering.

2. Scattering formalism

In this section expressions will be derived for the first- and second-order correlation functions of the doubly-scattered depolarised field.

Consider a sample consisting of a monodisperse solution of optically isotropic spherical particles with polarisability α. They are Rayleigh–Gans scatterers with a form factor $f(q)$ depending on the magnitude of the scattering vector $\boldsymbol{q}$ and defined by

$$f(q) = v^{-1} \int_{\text{particle}} \exp(\mathrm{i}\boldsymbol{q} \cdot \boldsymbol{r})\, \mathrm{d}\boldsymbol{r}$$

with v the volume of the particle. We assume that the particles are moving independently of each other and that they have a translational diffusion coefficient D_T and a rotational diffusion coefficient D_R. The sample is illuminated by a laser beam described by

$$\boldsymbol{E}_0(\boldsymbol{r}, t) = \hat{\boldsymbol{n}}_i \mathscr{E}(\boldsymbol{r}) \exp(\mathrm{i}\boldsymbol{k}_i \cdot \boldsymbol{r} - \mathrm{i}\omega\tau)$$

where $\mathscr{E}(\boldsymbol{r})$ describes the spatial beam profile and $\hat{\boldsymbol{n}}_i$ is a unit vector specifying the polarisation. The scattered light with wavevector $\boldsymbol{k}_f$ and polarisation $\hat{\boldsymbol{n}}_f$ passes through a system of pinholes and is detected by a photomultiplier. The pinholes admit light with a spatial profile $\mathscr{D}(\boldsymbol{r}) \cdot \mathscr{D}(\boldsymbol{r})$ is defined as the factor by which the field scattered at $\boldsymbol{r}$ is attenuated before it reaches the photomultiplier. The functions $\mathscr{D}(\boldsymbol{r})$ and $\mathscr{E}(\boldsymbol{r})$ define the scattering volume, which we assume to be large compared with the wavelength.

Now consider a process where light is first scattered by particle l at $\boldsymbol{r}_l$ and subsequently by particle λ at $\boldsymbol{r}_\lambda$ (see figure 1). The field at $\boldsymbol{r}_\lambda$ due to the scattering by particle l is given by (Berne and Pecora 1976)

$$\begin{aligned}\boldsymbol{E}_s(\boldsymbol{r}_\lambda, t) &= \alpha k_i^2 f(q_l)[\hat{\boldsymbol{n}}_i - (\hat{\boldsymbol{n}}_i \cdot \hat{\boldsymbol{r}}_{l\lambda})\hat{\boldsymbol{r}}_{l\lambda}]\, \mathscr{E}(\boldsymbol{r}_l)(\epsilon_0 r_{l\lambda})^{-1} \exp[\mathrm{i}(\boldsymbol{q}_l \cdot \boldsymbol{r}_{l\lambda} + \boldsymbol{k}_i \cdot \boldsymbol{r}_\lambda - \omega t)] \\ &= \mathscr{E}(\boldsymbol{r}_l)\boldsymbol{T}(\lambda, l) \cdot \hat{\boldsymbol{n}}_i f(q_l) \exp[\mathrm{i}(\boldsymbol{q}_l \cdot \boldsymbol{r}_{l\lambda} + \boldsymbol{k}_i \cdot \boldsymbol{r}_\lambda - \omega t)] \qquad (1)\end{aligned}$$

$$\boldsymbol{T}(\lambda, l) \equiv \alpha k_i^2 [\mathbf{1} - \boldsymbol{r}_{l\lambda}\boldsymbol{r}_{l\lambda}]/\epsilon_0 r_{l\lambda}$$

where we have used $\boldsymbol{r}_{l\lambda} = \boldsymbol{r}_\lambda - \boldsymbol{r}_l$, $\boldsymbol{k}_{l\lambda} = k_i \hat{\boldsymbol{r}}_{l\lambda}$ and $\boldsymbol{q}_l = \boldsymbol{k}_{l\lambda} - \boldsymbol{k}_i$. Equation (1) is the long-distance approximation for dipole radiation. The contribution of the short-distance part to the scattered intensity is negligible when particle dimensions are of the order of the wavelength.

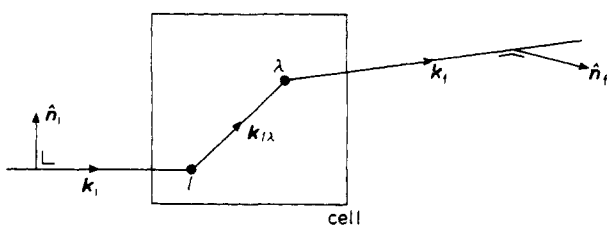

Figure 1. Double scattering by two particles l and λ.

The field on the detector surface at $\boldsymbol{r}_P$ with polarisation $\hat{\boldsymbol{n}}_f$ due to subsequent scattering by particle λ is given by

$$E_d(\boldsymbol{r}_P, t) = (\hat{\boldsymbol{n}}_f \cdot \boldsymbol{T}(P, \lambda) \cdot \boldsymbol{T}(\lambda, l) \cdot \hat{\boldsymbol{n}}_i) f(q_l) f(q_\lambda) \exp(i\boldsymbol{q}_l \cdot \boldsymbol{r}_{l\lambda} + i\boldsymbol{q}_\lambda \cdot \boldsymbol{r}_{\lambda P}) \times \mathscr{E}(\boldsymbol{r}_l)\mathscr{D}(\boldsymbol{r}_\lambda) \exp(i\boldsymbol{k}_i \cdot \boldsymbol{r}_P - i\omega\tau) \equiv B_{l\lambda}(t) \exp(i\boldsymbol{k}_i \cdot \boldsymbol{r}_P - i\omega\tau)$$

with $\boldsymbol{q}_\lambda = \boldsymbol{k}_f = \boldsymbol{k}_{ld}$ and $\boldsymbol{r}_{\lambda P} = |\boldsymbol{r}_P - \boldsymbol{r}_\lambda|$. As only the depolarised component will be considered, $\hat{\boldsymbol{n}}_f \cdot \hat{\boldsymbol{n}}_i = 0$. Summation over all pairs l and λ in the sample yields

$$E_d(\boldsymbol{r}_P, t) = \sum_{l \neq \lambda} B_{l\lambda}(t) \exp(i\boldsymbol{k}_i \cdot \boldsymbol{r}_P - i\omega\tau).$$

The first-order correlation function of the field at $\boldsymbol{r}_P$ is given by

$$C_1^d(\tau) = \langle E_d^*(\boldsymbol{r}_P, 0) E_d(\boldsymbol{r}_P, \tau) \rangle = \left\langle \sum_{l \neq \lambda} \sum_{m \neq \mu} B_{m\mu}^*(0) B_{l\lambda}(\tau) \right\rangle \exp(-i\omega\tau). \tag{2}$$

If the distances between particles are long compared with the wavelength, the functions $\boldsymbol{T}$, $f(q_l)$, $f(q_\lambda)$, $\mathscr{E}(\boldsymbol{r}_l)$ and $\mathscr{D}(\boldsymbol{r}_\lambda)$ in $B_{l\lambda}$ vary slowly in time compared with the rapidly fluctuating phase factors. We therefore assume that these functions are constant in equation (2). The contribution of scattering events for which this assumption does not hold can be neglected if the dimensions of the scattering volume are large compared with the wavelength. This will most often be the case in experimental set-ups.

From the terms in equation (2) only those with $l = m$ and $\lambda = \mu$ contribute to the correlation function, since the other terms cancel in the process of averaging. Substituting

$$\langle \exp[i\boldsymbol{q}_l \cdot \boldsymbol{r}_l(0) - i\boldsymbol{q}_l \cdot \boldsymbol{r}_l(\tau)] \rangle = \exp(-D_T q_l^2 \tau)$$

into equation (2) we obtain the first-order correlation function

$$C_1^d(\tau) = \sum_{l\lambda} |B_{l\lambda}(0)|^2 \exp(-D_T q_l^2 - D_T q_\lambda^2 \tau - i\omega\tau). \tag{3}$$

To obtain the second-order correlation function $C_2^d(\tau)$ from $C_1^d(\tau)$ the Siegert relation may be used provided the scattered field has gaussian statistics (Glauber 1963). For the practical geometries we use, the field produced on the second scatterer by the first scattering process is spatially incoherent (Van Rijswijk and Smith 1976). In that case the doubly-scattered field has gaussian statistics and

$$C_2^d(\tau) = 1 + |C^d(\tau)|^2.$$

3. Computations

In order to calculate $C_1^d(\tau)$ and $C_2^d(\tau)$ explicitly the sum in equation (3) is converted to a sixfold integral over the sample volume. This integral is easily computed for a gaussian beam and detection profile, defined by

$$\mathscr{E}^2(\boldsymbol{r}) = \frac{P_0}{2\pi r_E^2} \exp(-r_b^2/2r_E^2) \qquad \mathscr{D}^2(\boldsymbol{r}) = \exp(-r_f^2/2r_D^2). \tag{4}$$

Here r_b is the distance between $\boldsymbol{r}$ and the beam axis (z axis) and r_f is the distance between $\boldsymbol{r}$ and the detection axis in the x–z plane (see figure 2). When the scattering angle θ_f is zero these axes are collinear. This means that the intensity of the beam in a plane perpendicular to the beam is gaussian with the e^{-2} point at a distance r_E from the axis of the beam. The detector accepts only light of wavevector $\boldsymbol{k}_f$ with a detection efficiency $\mathscr{D}^2$, which depends on the distance r_f to the detector axis. r_D may be looked upon as the radius of the detected beam. P_0 is the incident light power. Cell dimensions are taken to be infinite for ease of computation.

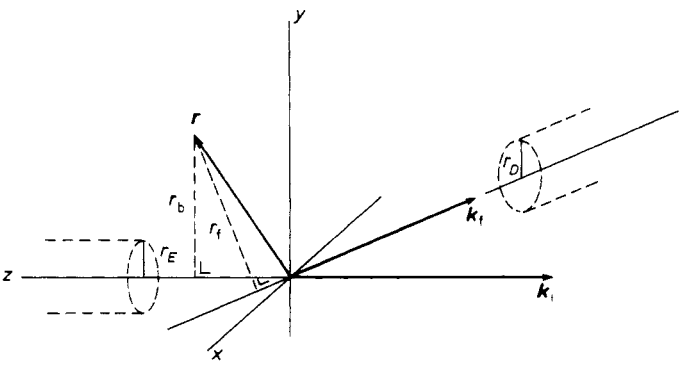

Figure 2. Coordinates used in equation (4) to specify beam and detection profiles $\mathscr{E}$ and $\mathscr{D}$. The profiles are indicated by broken lines.

The integral mentioned above is determined by the convolution of $\mathscr{E}^2$ and $\mathscr{D}^2$ (denoted by $\mathscr{E}^2 * \mathscr{D}^2$) as $\boldsymbol{T}(\lambda, l)$ and the form factors depend only on $\boldsymbol{r}_{l\lambda}$ (c_n denotes the number density of scatterers):

$$S_1^d(\tau) = \int d\boldsymbol{r}_l\, d\boldsymbol{r}_\lambda c_n^2 \mathscr{E}^2(\boldsymbol{r}_l)\mathscr{D}^2(\boldsymbol{r}_\lambda)(\hat{\boldsymbol{n}}_i \cdot \boldsymbol{T}(P,\lambda) \cdot \boldsymbol{T}(\lambda, l) \cdot \hat{\boldsymbol{n}}_f)^2 f^2(q_l) f^2(q_\lambda)$$
$$\times \exp[-D_T(q_l^2 + q_\lambda^2) - i\omega\tau]$$
$$= \int d\boldsymbol{r}_{l\lambda} c_n^2 (\mathscr{E}^2 * \mathscr{D}^2)(\boldsymbol{r}_{l\lambda})(\hat{\boldsymbol{n}}_i \cdot \boldsymbol{T}(P,\lambda) \cdot \boldsymbol{T}(\lambda, l) \cdot \hat{\boldsymbol{n}}_f)^2 f^2(q_l) f^2(q_\lambda)$$
$$\times \exp[-D_T(q_l^2 + q_\lambda^2) - i\omega\tau]. \tag{5}$$

For scattering at an angle $\theta_f \neq 0$ (see figure 3) we find from (4) with Fourier analysis that

$$(\mathscr{E}^2 * \mathscr{D}^2)(\boldsymbol{r}) = \frac{P_0}{|\sin\theta_f|} \frac{2\pi r_D^2}{[2\pi(r_D^2 + r_E^2)]^{1/2}} \exp[-y^2/2(r_E^2 + r_D^2)]$$

(y denotes the component of $\boldsymbol{r}$ along the y axis). For $\theta_f = 0$ we compute $C_1^d(\tau)$ and $\mathscr{E}^2 * \mathscr{D}^2$ per unit cell length in order to get a finite result:

$$(\mathscr{E}^2 * \mathscr{D}^2)(\boldsymbol{r}_{l\lambda}) = P_0 \frac{r_D^2}{r_D^2 + r_E^2} \exp[-r_{l\lambda}^2 \sin^2\theta/2(r_E^2 + r_D^2)]$$

where θ is the angle between $\boldsymbol{r}_{l\lambda}$ and the beam axis (see figure 3). The integrand of (5)

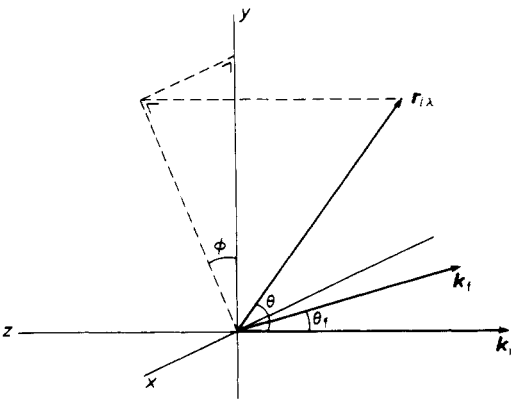

Figure 3. Coordinate system used in the computation of $C_2^d(\tau)$. ϕ and θ are polar coordinates of $r_{l\lambda}$ around k_i.

can now be evaluated in polar coordinates around k_i, namely $r_{l\lambda}$, θ and ϕ:

$$q_l^2 = 2k_i^2(1-\cos\theta)$$

$$q_\lambda^2 = 2k_i^2(1+\sin\phi\,\sin\theta\,\sin\theta_f-\cos\theta\,\cos\theta_f)$$

$$\hat{n}_i \cdot T(P,\lambda)\cdot \boldsymbol{T}(\lambda,l)\cdot \hat{n}_f = \cos\phi\,\sin\theta(\sin\theta\,\sin\theta\,\cos\theta_f+\cos\theta\,\sin\theta_f)\frac{\alpha^4 k_i^8}{r_{\lambda l}R}.$$

R is the distance between the sample and the photomultiplier, which is assumed to be large compared with real cell dimensions.

The form factor f is known analytically for spheres of radius a:

$$f(q) = \frac{3}{(qa)^3}(\sin qa - qa\cos qa),$$

whereas for Rayleigh–Gans scatterers the usual approximation

$$f^2(q) = 1-\tfrac{1}{3}q^2R_G^2$$

may be taken. R_G denotes the radius of gyration. The integration over $r_{l\lambda}$, and for $\theta_f = 0$ also over ϕ, can be performed analytically. For $\theta_f = 0$ the result is

$$C_1^d(\tau) = \frac{2\pi^2 r_D^2 P_0 \alpha^4 k_i^8 c_n^2}{8\epsilon_0^4 R^2[2\pi(r_D^2+r_E^2)]^{1/2}}\int \sin^4\theta\, f^4(q_l(\theta))\exp[-4D_T k^2\tau(1-\cos\theta)-i\omega\tau]\,d\theta. \tag{6}$$

This formula and the corresponding one for $\theta_f \neq 0$ are easily implemented on a computer. Typical results are shown in figures 4 and 5, together with experimental data on polystyrene latex spheres that will be discussed in § 5.

In order to check whether the time dependence of the correlation functions is influenced by the shape of the beam and detection profile, we considered another geometry for $\theta_f = 0$. In this 'cylindrical' geometry $\mathscr{E}(\mathbf{r})$ and $\mathscr{D}(\mathbf{r})$ are constant within a

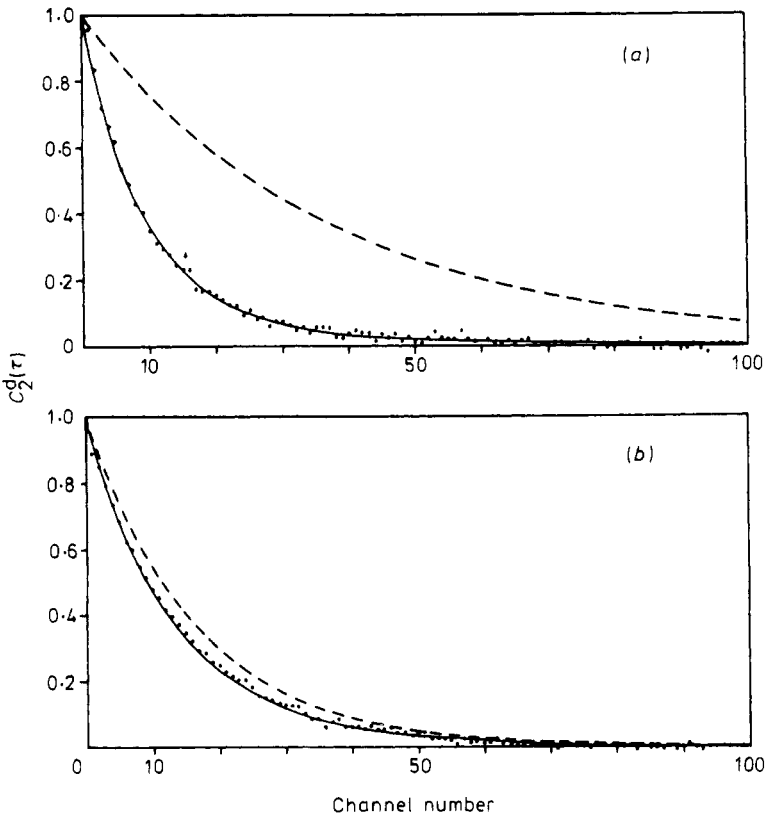

Figure 4. Double-scattering correlation function $C_2^d(\tau)$ against delay channel for latex spheres of 0·091 μm diameter in water at 19·6 °C. Only the AC part of the correlation function is shown. The full curve is computed with $D_T = 4{\cdot}7 \times 10^{-8}$ cm^2 s^{-1}. For comparison, the curve corresponding to $\exp(-2D_T q^2 \tau)$ is also shown (broken curve). (*a*) $\theta_f = 56{\cdot}7°$, τ = channel number × 10 μs, concentration = 1×10^{-4} in volume; (*b*) $\theta_f = 122°$, τ = channel number × 20 μs, concentration = 1×10^{-4} in volume.

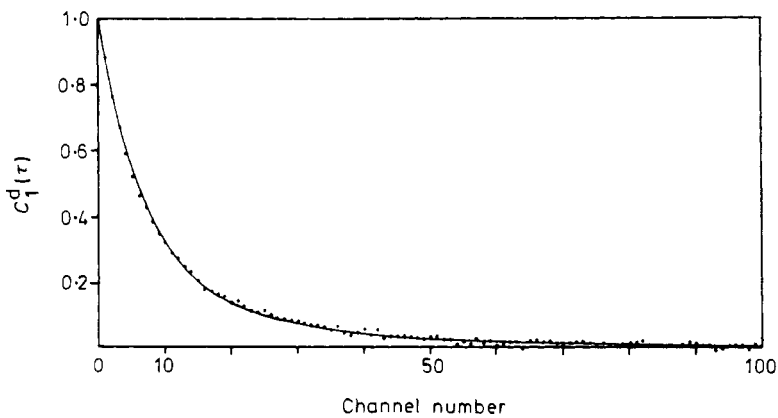

Figure 5. Depolarised double-scattering correlation function $C_1^d(\tau)$ for latex spheres of 0·109 μm diameter in water at 22 °C. The full curve is computed with $D_T = 4 \times 10^{-8}$ cm^2 s^{-1}, $\theta_f = 0$. Concentration is 1×10^{-4} in volume.

radius r_E and r_D from the z axis (see figure 2):

$$\mathscr{E}^2(\boldsymbol{r}) = \frac{P_0}{\pi r E^2} \qquad \text{if } r_b \leqslant r_E$$
$$= 0 \qquad \text{if } r_b > r_E$$
$$\mathscr{D}^2(\boldsymbol{r}) = 1 \qquad \text{if } r_b \leqslant r_D$$
$$= 0 \qquad \text{if } r_b > r_E.$$

The scattering volume has a length l. The integral for $C_1^d(\tau)$ was reduced to a threefold integral and thus evaluated numerically. Correlation functions computed in this way differ significantly from correlation functions computed with corresponding gaussian geometries only if the cell length l is of the order of r_E and r_D. In general, it appears that for $l \gg r_E$, r_D the time dependence of $C_1^d(\tau)$ is independent of geometry, while $C_1^d(0)$ is proportional to l (figure 6). This is due to the fact that the amount of double scattering is determined by the factor $\sin^4\theta$ in equation (6). The main contribution to the integral therefore arises from values of θ around $\frac{1}{2}\pi$, where $r_{l\lambda}$ is roughly perpendicular to $\boldsymbol{k}_i$.

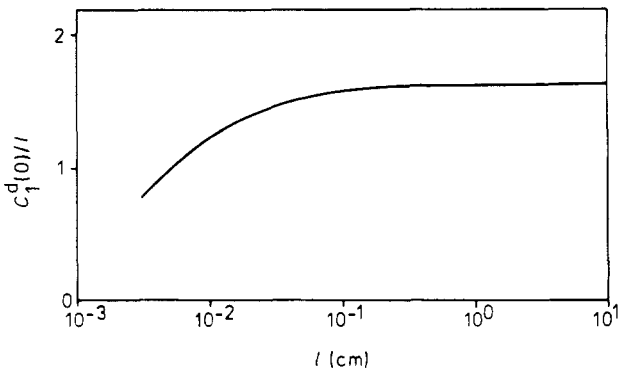

Figure 6. Plot of $C_1^d(0)/l$ (arbitrary scale) against l for a cylindrical geometry with $r_E = r_D = 0{\cdot}01$ cm, $\theta_f = 0$.

4. Measurement of rotational diffusion coefficients

If the particles have an optical anisotropy β, there is also a depolarised field due to single scattering. The correlation function of this field, $C_1^s(\tau)$, may be used to determine the rotational diffusion coefficient D_R of the scatterers. Therefore we want to know the ratio $C_1^d(0)/C_1^s(0)$. For $\theta_f = 0$ the function $C_1^s(\tau)$ may be computed per unit cell length using a depolarisation ratio $\beta^2/15\alpha^2$ (see, e.g., Berne 1977, p 154):

$$C_1^s(\tau) = \int \mathscr{D}^2(\boldsymbol{r}_l)\mathscr{E}^2(\boldsymbol{r}_l)\frac{\beta^2}{15}\frac{k_i^4}{\epsilon_0^2 R^2}\exp(-6D_R\tau)c_n \, d\boldsymbol{r}_l$$
$$= \frac{r_D^2}{r_E^2 + r_D^2} P_0 c_n \frac{k_i^4}{\epsilon_0^2 R^2}\frac{\beta^2}{15}\exp(-6D_R\tau). \qquad (7)$$

If $\beta^2/15\alpha^2 \ll 1$ the contribution of the anisotropy to polarised single scattering is negligible, so (6) remains valid. From (6) and (7) we infer

$$C_1^d(0)/C_1^s(0) \sim (r_E^2 + r_D^2)^{1/2} c_n. \tag{8}$$

A straightforward proof can be given that this equation also holds for $\theta_f \neq 0$. If one wishes to determine the rotational diffusion coefficient from the correlation function of the depolarised field one has to minimise the ratio (8). It is clear that this can be done by taking c_n small and $r_E \simeq r_D$, whereas both should be taken as small as possible. When $r_D \ll r_E$ the signal-to-noise ratio would be reduced significantly while $C_1^d(0)/C_1^s(0)$ is not reduced very much.

5. Experimental

Measurements of depolarised light scattering in the forward direction and at an angle were performed with separate instruments. The arrangement of the optics was the same in both instruments, and is depicted in figure 7. The sample is illuminated with typically 100 mW light from an argon-ion laser operating at 514 nm. Lens L_1 focusses the incident light on the sample and lens L_2 images the pinhole A_2 at the focus of lens L_1. The polariser–analyser system used had a transmission of about 3×10^{-7}. Lenses and pinholes can be chosen in such a way that the optimum conditions for the measurement of rotational diffusion coefficients from single depolarised scattering are realised.

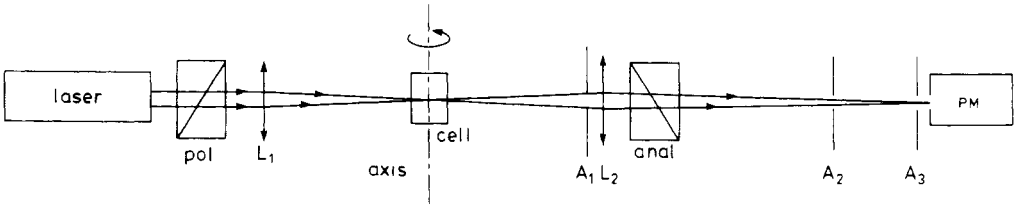

Figure 7. Arrangement of the optics. L_1, L_2 are lenses, A_1, A_2, A_3 are apertures, PM is the photomultiplier, anal is the analyser and pol the polariser.

Due to diffraction the scattering geometry is reasonably well described by (4). As has been shown in § 3, deviations from this geometry will influence only the magnitude of the correlation function provided that the cell length is sufficiently large. r_D is determined by the magnitude of the image of pinhole A_2. r_E depends on the focal length of L_1 and the diameter of the beam coming from the laser. Their values are approximately $r_E = 50$ μm, $r_D = 75$ μm for $\theta_f \neq 0$ and $r_E = 65$ μm, $r_D = 200$ μm for $\theta_f = 0$.

To be able to measure double-scattering correlation functions r_D and r_E were taken larger than necessary for $\theta_f = 0$. The cell length was taken to be 1 cm for $\theta_f = 0$. Figure 6 shows that $C_1^d(0)/C_1^s(0)$ should be independent of cell length for large l. In practice, however, this ratio decreases with l, e.g. as a consequence of the divergence of the beam. $l = 1$ cm is a reasonable compromise when $r_E = 65$ μm.

The scattered light was detected by RCA 8850 PM tubes. The photomultiplier output was analysed by a Malvern clipping correlator for $\theta_f \neq 0$. In the forward direction the light transmitted by the polariser–analyser system causes heterodyne detection. In spite of the transmission of 3×10^{-7}, the local oscillator intensity is so high that analogous correlation is necessary. Therefore an HP 3721 A correlator has been used.

We measured double-scattering correlation functions for a suspension of polystyrene latex spheres in water. The spheres had diameters of 0·091 μm and 0·109 μm and a relative refractive index of 1·19 (Tschudi *et al* 1975). Approximately, they may be regarded as Rayleigh–Gans scatterers at a wavelength of 514 nm. Concentrations were taken such that triple scattering was negligible (1×10^{-4} in volume). This was checked by measuring the concentration dependence of the magnitude of the correlation functions. Although careful precautions were taken against contamination by dust, the measurements always yielded correlation functions that were slightly shifted towards higher values. This may be attributed to slow fluctuations in the local oscillator intensity. We therefore subtracted a constant background from the experimental data. The data were normalised to unity at $\tau = 0$ and plotted together with calculated curves. The values of D_T used in the calculations that give a correct fit differ by less than 1% from those obtained from the Stokes formula. Some results are given in figures 4 and 5. An excellent agreement between theory and experiment exists.

6. Conclusions

In the measurement of rotational diffusion coefficients by depolarised light scattering spectrometry, difficulties must be expected due to double-scattering effects. These effects may be minimised by reducing the particle concentration as much as possible and by using an appropriate geometry. Such a geometry was proposed in figure 7. It was shown that an optimum choice is $r_E \sim r_D$ with both as small as possible. For the forward direction the cell length should be chosen in such a way that the beam diameter does not increase too much by divergence as this increases the ratio $C_1^d(0)/C_1^s(0)$. A good compromise is $l = 1$ cm if $r_D = 60$ μm.

If it is not possible to remove the double-scattering effects completely by choosing a low concentration and optimum geometry, corrections may be calculated. Explicit expressions for the double-scattering correlation functions were derived for gaussian geometries. Comparison between a cylindrical and a gaussian geometry in the case of the forward direction showed that the time dependence of the double-scattering correlation functions is not noticeably influenced by details of beam and detection profile if $l \gg r_E, r_D$. The correlation functions computed numerically were compared with experiment for the case of polystyrene latex spheres. The results in figures 3 and 4 show an excellent agreement between experiment and theory.

If the decay times of $C_1^s(\tau)$ and $C_1^d(\tau)$ are of the same order of magnitude, it is essential to exclude double scattering. The feasibility of a measurement of $C_1^s(\tau)$ may now in principle be inferred from equations (6) and (7) when α and β are known. For T4B phages, for example, exclusion is only possible at a concentration at which it is too low to measure $C_1^s(\tau)$ (Hopman *et al* 1978).

If the decay times of $C_1^s(\tau)$ and $C_1^d(\tau)$ differ sufficiently, $C_1^s(\tau)$ and $C_1^d(\tau)$ may be distinguished using double-scattering correlation functions calculated numerically.

Acknowledgment

We wish to thank Professor Dr Blok for many fruitful discussions during the completion of this work.

References

Berne B J and Pecora R 1976 *Dynamic Light Scattering* (New York: Wiley)
Hopman P C, Koopmans G and Greve J 1978 to be submitted to *Biopolymers*
Glauber R J 1963 *Phys. Rev.* **131** 2766–88
Sorensen C M, Mockler R C and O'Sullivan W J 1976 *Phys. Rev.* A **14** 1520–32
Tschudi T, Rohrbach P and Herziger G 1975 *Optik* **43** 175–83
Van Rijswijk F C and Smith U L 1976 *Physica* **83A** 121–42